Acta Geotechnica (2025) 20:2075–2092
https://doi.org/10.1007/s11440-025-02603-0

RESEARCH PAPER

Effects of soil saturation and suction on root reinforcement performance: pull-out experiments on six native Australian plants

Jiale Zhu[1] · Abbas El-Zein [1] · Thomas C. T. Hubble [2] · Guien Miao[1]

Received: 14 June 2024 / Accepted: 7 March 2025 / Published online: 27 March 2025

Abstract
Improving shallow slope stability with vegetation requires an understanding of root reinforcement performance, in addition to consideration of local ecological impacts. Existing root reinforcement models have not accounted for the influence of soil water content, due to insufficient experimental evidence and theoretical understanding. In this study, the root reinforcement behaviour of six Australian native plants (*A. costata*, *B. integrifolia*, *E. reticulatus*, *P. incisa*, *C. citrinus* and *M. thymifolia*) are examined through vertical pull-out tests under various levels of volumetric water content (VWC) and suction. Additionally, this study employed two root reinforcement models to illustrate the impact of VWC on comparing the performance of these models with experimental results. The study also employs an innovative approach by making an analogy to soil nails or piles and normalising pull-out force against the peripheral surface area of root-soil bundles, defining this as pull-out stress. The results show that VWC and suction have a strong influence on reinforcement, with a roughly linear inverse relationship observed between VWC and pull-out force of root bundles recorded for all species. The pull-out stress followed a nonlinear inverse relationship with VWC and suction as the pull-out force. Furthermore, discrepancies between established-model predictions and experimental data widen with increasing VWCs. It is also found that inadequate sampling can also lead to substantial errors in estimating the actual water content of the soil. The study demonstrates that VWC and suction significantly impact root reinforcement performance, with pull-out strength decreasing as VWC increases. The study also highlights the importance of accurately recording soil water content in root reinforcement experiments and modelling.

Keywords Native Australian flora · Pull-out test · Root reinforcement model · Slope reinforcement · Unsaturated soil

1 Introduction

Shallow landslides typically involve slope material with a depth of less than 2 m and can involve up to 1000 m^3 of soil, travelling through mechanisms of sliding, flowing and complex movement [1]. It has been long recognised that vegetation enhances soil mass strength and generally improves hillslope's stability through various mechanisms. These include mechanical strengthening of the soil; anchoring within the soil failure plane; and reducing the soil water content to enhance soil strength [2–7].

Investigations of the mechanical interaction between roots and soil have mostly gathered experimental data acquired by direct shear tests [8, 9], root tensile tests [10, 11] and pull-out tests [12, 13]. These three methods provide information on root reinforcement behaviour from different perspectives. For instance, the direct shear tests explore the additional cohesion provided by roots in comparison to unrooted soil [8], while root tensile tests provide information on the physical properties of roots [14]. The pull-out of root (bundles) is also effective as it simulates and estimates the root-soil bundle response in tensile-loading situations [13]. Mechanical reinforcement of soil by roots can be provided in several modes. Firstly, trees with deep roots anchor a slope mechanically like constructed soil nails or piles that convert the shear force

✉ Jiale Zhu
jiale.zhu@sydney.edu.au

[1] School of Civil Engineering, The University of Sydney, Shepherd St, Darlington, NSW 2008, Australia

[2] School of Geosciences, The University of Sydney, City Road, Camperdown, NSW 2006, Australia

between basal failure surfaces in the soil into tension in the tree roots. Secondly, lateral roots are found to provide a resisting tensile stress near the surface hence conferring additional tension or compression strength around a landslide's scarp or toe [4, 15]. Finally, during a windstorm, uprooting from the wind can transmit uprooting tensions to the tree-embedded soil [16]

Prior investigations have tended to focus on horizontal pull-out experiments on individual roots [e.g. 17, 18, 19], or on root bundles or analogues in remoulded soil [e.g. 20, 21, 12, 22], in which the pull-out direction has been parallel to the plane of the slope. These studies have shown that pull-out resistance is influenced by root tensile strength, root elastic modulus and geometric factors such as branching. In contrast, experiments focusing on vertical pull-out, i.e. perpendicular to the plane of the slope, especially at the scale of an entire tree root system, are relatively scarce and preliminary [13, 23–25]. The lack of vertical pull-out studies can be attributed to the time-consuming process of growing appropriated sized plant samples [26], and the difficulty of deploying equipment capable of uprooting mature trees or testing in a sufficiently controlled manner.

Given that the main strong roots of trees penetrate through the failure plane in a manner akin to soil nails or piles, it is reasonable to employ an experimental method commonly used for strength evaluation of these two artificial geo-reinforcement structures, such as vertical pull-out test. This is the rationale for using measurements of vertical pull-out force as a quantitative measure of a plant's ability to stabilise slopes [24, 27, 28]. These experiments involve extracting individual plants while minimising disturbance to the surrounding soil [29]. Furthermore, the results can provide valuable data for root reinforcement models, such as the load–displacement curve for strain-based progressive failure in the root bundle model (RBM) [4]. Ultimately, vertical pull-out tests are recommended for evaluating resistance, as they measure the lower threshold of pull-out strength, thus ensuring a safe margin in slope design [30, 31].

In addition to the mechanical reinforcement, the reduction of water content in slope also plays an important role in enhancing the slope stability [6]. This hydrological effect includes increased transpiration and improved infiltration regulation, both of which contribute to improved slope stability [32, 33]. However, current root reinforcement models often assume that the strength of reinforced soil is a function of root properties, with the ultimate breakage failure of individual roots in a bundle as the primary factor [34]. Previous studies have generally attributed a constant value to plant-conferred strength. However, the effects of soil matrix conditions, especially volumetric water content (VWC) and matric suction, have not been adequately incorporated into these models or experiments [4, 22, 31, 35, 36]. The absence of this factor can introduce discrepancies between model-calculated results and actual (experimental) results. For instance, Zhu et al [22] and Wang et al. [37] found that the interfacial friction between soil and roots weakens with the increase of soil water content which may have resulted in roots slipping before they break. Such shifts in root-soil failure patterns were also observed by Zhang et al. [31] during pull-out tests on small plants in sandy soils. The change from root breakage to slippage may invalidate the assumption of ultimate breakage in the current root reinforcement models [e.g. 38, 39, 40].

It is usual for the impact of soil water content on reinforcement performance to be considered in pull-out studies of other forms of constructed reinforcements, such as piles [41, 42], soil nails [43–46] and geotextiles [47, 48]. It is therefore reasonable to apply the same data acquisition protocols for bio-reinforcement materials as this more nuanced investigation of pull-out behaviour in unsaturated soils will undoubtedly enhance our understanding of the behaviour of root-reinforced soils.

In root-soil experiments, soil water content and suction are often not considered critical variables for control or measurement. However, results obtained under otherwise identical conditions can vary significantly due to differences in soil water content caused by precipitation or variation in drainage conditions. Existing models do not account for the effects of soil water content on root reinforcement performance, partly because these effects have not been adequately researched and hence are not well understood. This gap may be attributed to the limited effects of soil water content observed in pull-out tests on individual root analogues [12]. Furthermore, controlling and accurately measuring soil water content is challenging, particularly in larger-scale in situ experiments, as noted by Docker and Hubble [8]. It is also possible that the emphasis on tensile failure in current models contributes to this oversight, where the interaction between soil and roots is not considered. Although some studies have presented soil water content or suction as factors that influence root reinforcement [e.g. 12, 31], many others have only approximated the water content [e.g. 13, 24, 23], uniformly hydrated soil before testing [8], or ignored the water content altogether [e.g. 25, 27]. Addressing this oversight is critical to improving the applicability and accuracy of root reinforcement models in real-world scenarios.

Lastly, there are very few studies of the root reinforcement behaviour of native Australian species [e.g. 8, 19, 49]. Determination of root reinforcement and modelling this behaviour in specific geographical regions requires an understanding of the properties of specific species of trees relevant to these regions [24]. It also requires that the

species possess evolutionary adaptability to their environments. As yet, there has been no attempt at studying the pull-out behaviour of native Australian plants and hence assess their potential in soil reinforcement.

The aim of this paper is to address the three above-discussed gaps, namely scarcity of vertical pull-out tests, lack of consideration of water content and suction in root-soil experiments and models and absence of data on reinforcement potential of native Australian species. First, a series of vertical pull-out experiments on six Australian tree species, under varying soil water contents, are conducted. The relationships between peak pull-out stress, VWC and soil suction are quantified and discussed. Finally, the effect of VWC on the accuracy of two commonly used root-soil reinforcement models is investigated using the results from the three tree species. The paper hence generate new theoretical and practical knowledge on the reinforcement potential of native Australian tree species and the effects of partial soil saturation on root reinforcement.

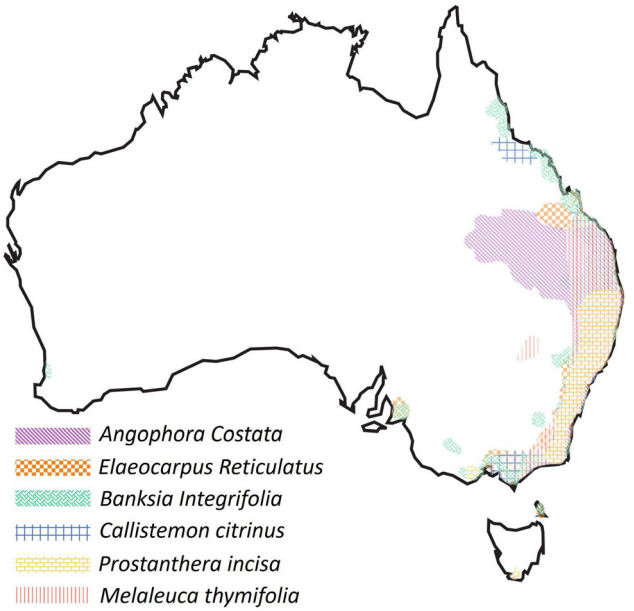

Fig. 1 Distribution map of *A. costata*, *E. reticulatus*, *B. integrifolia*, *C. citrinus*, *P. incisa* and *M. thymifolia*. Data collected from The Australasian Virtual Herbarium [56] and Australian National Botanic Gardens [50]

2 Methodology

2.1 Material used and experiment set-up

The species selections were based on botanical guidelines for native Australian vegetations [50–55]. The selection criteria for the selection of species account for ecological impacts and practitioner suggestions. The final selections were *Angophora costata* (*A. costata*), *Banksia integrifolia* (*B. integrifolia*) and *Elaeocarpus reticulatus* (*E. reticulatus*) for native tree species, and *Callistemon citrinus* (*C. citrinus*), *Prostanthera incisa* (*P. incisa*) and *Melaleuca thymifolia* (*M. thymifolia*) for native shrubs and ground cover. The total number of plant samples used in this study was 30, comprising 5 samples for 6 species to test at different water content levels.

The geographical distribution of these plants is shown in Fig. 1. The plants were initially collected from Randwick City Council Nursery. Randwick is an eastern suburb of Sydney (33°55' 9.16" S, 151°13' 28.17" E). The plants were about 12-month old at the time of collection (April 2021) and were cultivated for approximately another 18 months before the tests.

The trees and shrubs were set in 450 mm and 230 mm diameter pots, respectively, both with sandy soil containing organic matter (humus and wood chips). The organic content helped maintain soil moisture, inhibited insect infestation and kept a low level of nutrients to prevent excessive root growth, which can lead to root decay [57, 58]. Soil properties are shown in Table 1. From observation, the gravel-size materials were either wood pieces or agricultural perlite (SiO_2).

Table 1 Soil properties used in the pots

Soil property	Values	Units
Fines (<0.075 mm)	1.65	%
Sand (0.075–4.75 mm)	91.05	%
Gravel (>4.75 mm)	7.30	%
Specific gravity	2.12	
Friction angle	34.7	°
Dry density (undisturbed in the pots)	660	kg/m^3
Permeability	$2.3*10^{-3}$	mm/s
Organic matter	31.5	%

To find the diameter distribution of roots, four measurements of root were made at a vertical surface 100 mm away from the stem for each species using the reserved specimens. A 3D-printed 100 mm × 100 mm frame and a vernier calliper (0.01 mm accuracy) were used for the counting.

2.2 Pull-out apparatus

The laboratory pull-out apparatus used in this project accommodates both aforementioned pot sizes, by employing different of the steel legs on the bottom tier. Different sizes of confinement rings were used to stop the

relative movement between soil and the container wall. An example of the set-up is shown in Fig. 2 with the main components labelled. The ambient temperature and relative humidity were recorded.

Measuring and controlling water content in real-time were two key challenges in this root reinforcement study. A soil moisture sensor (MP406, ICT International) was employed to monitor the instantaneous VWC, which helped determine whether the specimen was ready for experiment with targeted VWC reached. Additionally, remote positioning tensiometers (2100F, ICT International) were used to measure the matric potential. The specimen was allowed to undergo evapotranspiration to decrease VWC and irrigated with water to increase it. Water content levels were chosen to represent field conditions from dry to near saturation. Five representative VWC levels were tested, with actual values measured and reported for analysis. Room temperature and humidity were measured before each test.

The water content in the soil can vary spatially and temporally due to seepage [59], evaporation [60] and plant transpiration [6, 61, 62]. Consequently, the water content is expected to be influenced by the spatial distribution of roots and their ability to absorb water, as well as the water retention properties of the soil. Many previous experiments [e.g. 24, 31, 30] presented the water content as a uniform value across the specimen. However, Garg et al. [61] found the suctions induced by the roots vary with depth, which consequently affects the soil water content.

To capture the spatial variation of VWC and suction in the 450 mm pots, measurements were obtained from four distinct locations. These locations were chosen to vary in terms of depth and lateral closeness to the plants, as depicted in Fig. 3. The containers for the tree samples were upside-down conical frustum pots with a top diameter of 450 mm, a bottom diameter of 400 mm and a height of 400 mm. The four monitoring points were located at 50 mm from the stem and 50 nm deep, 50 mm from the stem and 200 mm deep, 150 mm from the stem and 50 mm deep and 150 mm from the stem and 200 mm deep. These points were selected to capture spatial variations in VWC and suction. The representative value of VWC and suction for each pot was determined using the arithmetic mean of these four measurements. For the shrub specimens, given the container's dimensions, only two readings were taken: one at a depth of 5 cm and on at a depth of 20 cm, both at a distance of 5 cm from the stem. The representative VWC and suction values were then computed as the arithmetic mean of these two measurements.

Tree specimens were sawed 200 mm above the ground, while shrub specimens were cut down to maximum length possible for a secure connection with the pull-out apparatus. In previous experiments, it has been reported that the connection between the root and the pulling device was

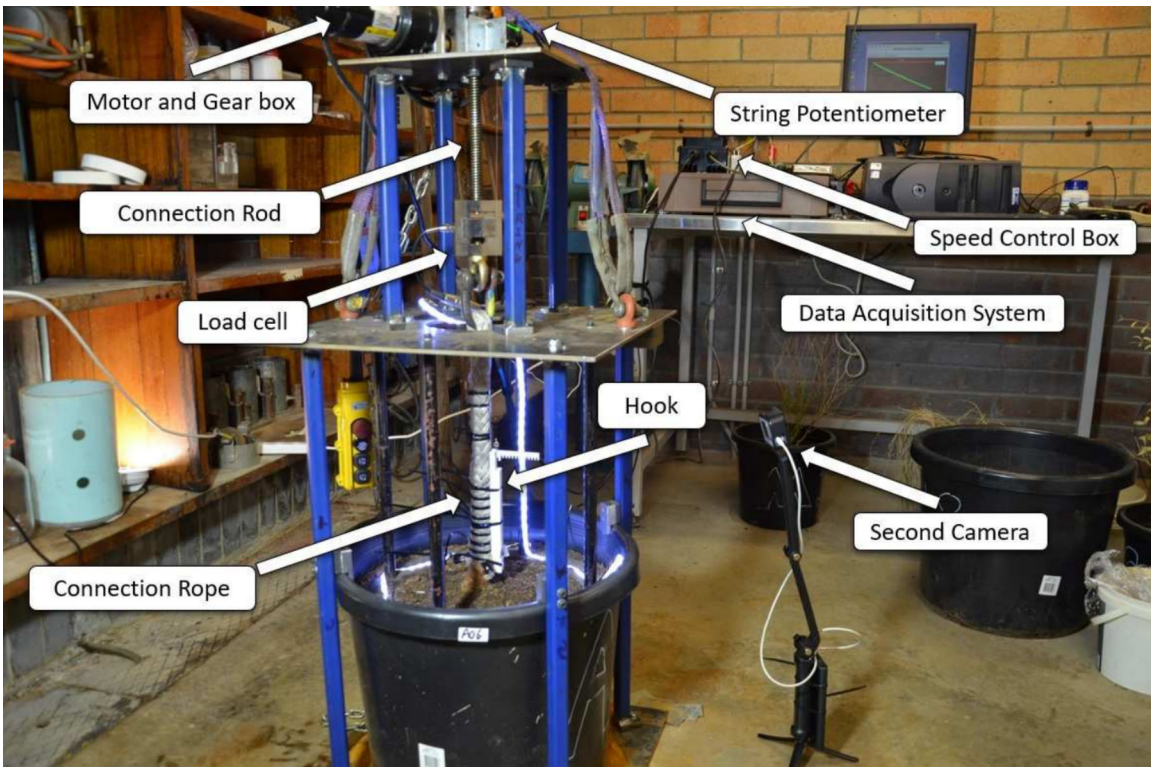

Fig. 2 Picture of the pull-out apparatus in experiment with main components labelled

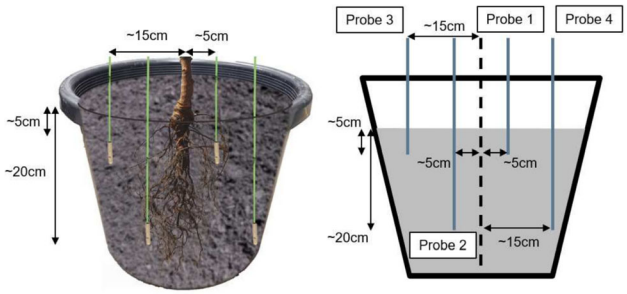

Fig. 3 Probe locations

sometimes too weak for an individual tree or induced excessive local transverse stress, leading to bark penetration and relative slip [26]. To address this, a hollow single-braid Dyneema rope was used to connect the remaining tree stem above the soil surface, employing a "Chinese finger-trap" mechanism. This rope applied evenly distributed pressure along the stem surface, offering high strength and low deformation to minimise displacement measurement errors. Before wrapping, the rope was compressed axially to create a hollow space, then wrapped around the stem and pulled tight for maximum contact. Zip ties were used along the length of the connection to prevent relative movement, as the rope would need to expand before sliding, which the zip ties constrained. A hook was attached to the exterior of the Dyneema rope to secure the ring from the string potentiometer, allowing accurate measurement of the displacement of the root bundle.

For the larger containers, a steel ring (inner diameter: 350 mm, outer diameter: 390 mm) was placed just above the ground to prevent movement between the soil and the pots. For the smaller containers, the ring had a dimension of 240 mm (outer) and 200 mm (inner). The pull-out speed was set to 0.1 mm/s. The pull-out speed of 0.1 mm/s was selected based on prior studies that tested a range of higher speeds, such as 2 mm/s in Norris [63] and 2.5 mm/s in Burrall et al. [13]. Finally, observations based on Cofie and Koolen [64] indicated that a speed of 0.1 mm/s would have minimal impact on results while allowing the experiment to be conducted within a practical time frame. The pull-out force, measured by the load cell, and displacement, measured using the string potentiometer, were recorded in real-time through a data acquisition system. The experiment was concluded once the travel distance (250 mm) was exhausted. The top section connected to the roots was then cautiously removed, and the bundle size with the soil matrix attached was recorded. The soil waste and vegetation remains were later used as fertiliser for the ground in the community compost bin.

2.3 Normalisation of the pull-out force

The pull-out capacity can vary between individual plants due to stochastic biological factors such as root dry mass, root diameter, cross-sectional area of rooted soil and the number of roots [65]. To enable better intra-species and inter-species comparison of performance, the pull-out force needs to be normalised to account for the difference in above-mentioned factors. Liu et al. [25] found that the broken soil area correlated well with the pull-out force of the root bundle. Building on this, Burrall et al. [13] suggested that a root system's resistance capacity can be related to how effectively the neighbouring soil is engaged with the root-soil bundle at the initial stage of loading. In this study, the roots all had relatively well-defined root-soil bundles, as displayed in Fig. 5. Therefore, the surface area of the root-soil bundle failure plane was used to normalise each peak pull-out force to account for the variation in bundle size.

When considering the root-soil matrix as a cylindrical bundle, the mechanical anchorage effect of tree roots in vertical pull-out tests parallels that of soil nails and rock bolts. The binding strength derived from lateral roots facilitates shaft friction between the root-soil bundle and the surrounding soil. Results from vertical pull-out tests, akin to axial pull-outs of micro-piles, can be used to evaluate the effectiveness of bioengineered slopes [27].

Each bundle was approximated as an elliptic cylinder, and the measured length of the shortest and longest axes were used, in conjunction with the depth (height), to calculate the surface area of the interface between root-soil bundle and the neighbouring soil. An idealised root-soil bundle is shown in Fig. 4.

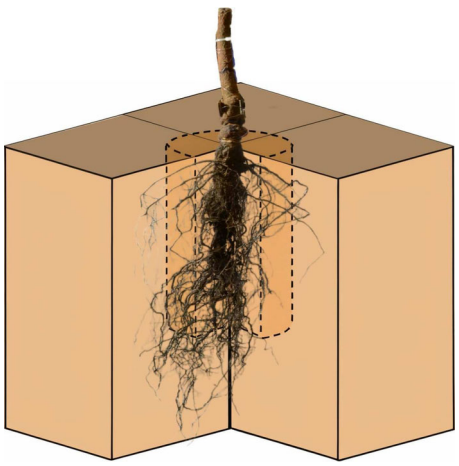

Fig. 4 An idealised cylindrical root-soil bundle formed by the main and finer roots. Illustration inspired by Ng et al [66]

2.4 Two root reinforcement models' application

In this study, the effect of root reinforcement by three tree species was estimated using two established models: the Wu-Waldron model (WWM) and the root bundle model Weibull (RBMw). Discrepancies between model predictions and experimental results under different soil moisture conditions were noted. The root reinforcement models were not applied to the three shrub species due to the lack of data on their root tensile properties. The WWM describes the maximum available reinforcement from the tensile strength of the roots by assuming simultaneous root breakage. In contrast, the RBMw emphasises the importance of force-displacement behaviour and incorporates a Weibull survival function to consider failure probability in complex systems Schwarz et al. [40]. For the use of RBMw, this study followed the refined methodology outlined in a case study research by Giadrossich et al. [14]. In both models, the root diameter distributions estimated from the experimental measurements were used. The roots were assumed to have a uniform cylindrical spatial distribution.

Before introducing the models, the tensile properties are first measured, as these are necessary inputs for the models. Tensile properties, including both tensile strength and stiffness, of roots from the three tree species were assessed using a Tinius Olsen H5KS ultimate tensile testing apparatus. The relationship between tensile strength and root diameter is widely accepted as a power-law relationship, where larger diameters correspond to lower tensile strengths. This has been demonstrated in numerous studies [e.g. 67, 68, 69, 70, 10, 71]. However, recent studies suggest that additional factors, such as root moisture content [72, 73] or cellulose degradation [74], may also influence tensile strength. Despite these findings, root diameter remains the most significant factor in characterising tensile strength, as shown by its consistent use in numerical models [34]. The relationship between tensile strength and diameter in this study was characterised using a power-law equation, aligned with methodologies employed in prior research that used the models introduced in this section. This approach ensures consistency with established practices. The power-law relationship is presented below.

$$F_{\max}(\phi_i) = k_1 \phi_i^{k_2} \tag{1}$$

Root stiffness is characterised by the secant elastic modulus, which is defined as the ratio of root strength to strain at failure [40]. In this study, the methodology proposed by Giadrossich et al. [14] was used, in which the secant elastic modulus is substituted with a spring constant to more directly represent the force-displacement relationship. The spring constant is defined as the relationship between the force and the change in displacement. The spring constant is dependent on root diameter through a power-law relationship, as indicated in Eq. 2.

$$k(\phi_i) = k_3 \phi_i^{k_4} \tag{2}$$

where k_3 is the spring constant as suggested in Schwarz et al. [40], and k_4 is the power-law exponent in the spring constant-diameter relationship.

Returning to the broader context of the model's application, the conventional WWM calculates the reinforcement effect as an additional stress term S_r

$$S_r = k' \times \sum (T_i \times RAR_i) \tag{3}$$

where T_i is the tensile strength in stress term (Pa) of individual root i, RAR_i is the root cross-sectional area ratio, which is the area of individual root i over an entire shear plane, and k' is a factor that accounts for the insertion angle effect on root reinforcement. The insertion angle effect k' is taken as 1 in this study [75, 76].

However, the RBMw reinforcement requires the result to be calculated as the sum of forces (N) activated by individual roots [14]. In this model, the nominal shear plane is considered to be a unit vertical cross-sectional cut, and stress (in Pa) is calculated by dividing the force by the area of this nominal surface plane. For better comparison, the conventional WWM expression is converted to calculate the maximum tensile force available per unit area using the tensile strength in force term (N), and the RAR is replaced by the number of roots (i.e. root density) of different root classes. The expression of WWM application in this study is shown below

$$F_{WWM} = \sum_{i=1}^{N} F_{max}(\phi_i) \tag{4}$$

where $F_{max}(\phi)$ is described with Eq. 1, and N is the total number of roots of different classes per unit area. As ϕ_i follows a discrete distribution, the median ϕ_i value of each class was taken for calculation same to Schwarz et al.'s (2013) [40] approach.

The core equation for RBMw estimate the total resistance force (F_{RBMw}) provided by the roots, in relation to displacement, through the following equation

$$F_{RBMw}(x) = \sum_{i=1}^{N} F(\phi_i, x) S(x^*) \tag{5}$$

where x is the displacement in mm, N is the total number of roots of different classes per unit area, $F(\phi_i, x)$ is the force of a single root with diameter ϕ_i at displacement x, and $S(x^*)$ is the Weibull survival function at normalised failure displacement x^*. The reinforcement from RBMw is subsequently expressed as total force F_{RBMw} per unit area.

The force of a single root with diameter ϕ_i at displacement x is estimated with the following equation

$$F(\phi_i, x) = k(\phi_i)x \tag{6}$$

The survival function follows a Weibull distribution

$$S(x^*) = e^{-\left(\frac{x^*}{k_5}\right)^{k_6}} \tag{7}$$

where x^* is the normalised failure displacement. k_5 is the shape factor, and k_6 is the scale factor that describes the probability function irrespective of the diameter, calibrated with experimental data. x^* is defined by

$$x^* = \frac{x}{x_{max}^{fit}(\phi_i)} \tag{8}$$

where $x_{\max}^{\text{fit}}(\phi_i)$ is defined by the power-law relationships in Eq. 1 and Eq. 2 as follows

$$x_{\max}^{\text{fit}}(\phi_i) = \frac{k_1}{k_3}\phi_i^{k_2-k_4} \tag{9}$$

The values of k_5 and k_6 in Eq. 7 were calibrated as described next. First, the experimental normalised failure displacements, x_{data}^*, were calculated with the following equation

$$x_{\text{data}}^* = \frac{x_{\max}^{\text{data}}}{x_{\max}^{\text{fit}}(\phi_i)} \tag{10}$$

where $x_{\max}^{\text{data}}$ is the experimentally measured displacement at failure, and $x_{\max}^{\text{fit}}(\phi_i)$ is fitted displacement at failure defined in Eq. 9. Then, the survival distribution value, S_i for each data point is calculated with

$$S_i = \frac{n_i}{N} \tag{11}$$

where n_i is the ranking of the roots in ascending order of x_{data}^*, and N is the total number of roots. The data from tensile tests were used to calibrate the parameters k_5 and k_6 by minimising the residual standard error between the distribution function S_i against x_{data}^* as shown in Sect. 3.5 Fig. 10. The calibration used a total of 31, 40 and 58 roots, respectively.

Table 2 Average root counts (integer) for the tree species in different diameter intervals at 100 mm from the stem. Diameters are categorised in mm

Species	$0<d<1$	$1<d<2$	$2<d<3$	$3<d<4$	$4<d<5$
A. costata	4	5	1	1	1
B. integrifolia	10	1	1	1	0
E. reticulatus	35	2	0	0	0

To calculate total maximum force F_{max}, root counts were conducted and categorised by diameter class as shown in Table 2. Using median diameters for each class, this discrete distribution was applied in Eq. 1. The same approach was adopted in Schwarz et al. [40].

In summary, the performance of WWM (τ_{WWM}) is evaluated using estimates of the density of roots of various diameter classes according to Eq. 1, which is further supplemented by Eq. 4 for a complete calculation. Meanwhile, the performance of the RBMw (τ_{RBMw}) uses the root density estimates along with Eq. 5, while integrating Eqs. 6 and 11 for evaluation. The peak reinforcement forces derived from each model were predicted from the number of roots per unit area and were subsequently articulated in terms of stress (kPa).

An adjustment factor, k'', is often employed in current root reinforcement model studies [34, 76, 77] to compare the later root reinforcement models with the original WWM. This factor is also used in this study. k'' is influenced by variables such as species and root spatial distribution [78], and is defined as the ratio of values obtained under alternate root reinforcement assumptions (in this study, τ_{RBMw}) to τ_{WWM}.

3 Results and discussion

3.1 Observation of the specimens

In all tests, the pulled-out bundle of root-soil matrix was found to be an approximate elliptic cylinder. Examples of elliptic-cylindrical bundles can be seen in Fig. 5. These observations are consistent with the findings of Burrall et al. [13], who found that root-soil matrices formed a central root-soil bulb or plate at failure. A test was considered successful if the root bundle fully detached from the surrounding soil by the end of this travel distance, which was the case for all samples. The two observed shapes of the root-soil bundles were determined by the fine roots' ability to grip surrounding soil particles but did not influence detachment.

The root diameter distribution helps describe the root architecture for use in calculations by reinforcement model. The diameters measured were separated into 1 mm interval, and the results are shown in Table 2. The table shows that the vast majority of roots in all three trees are less than 2 mm in diameter, with roots in B. integrifolia and E. reticulatus mostly less than 1 mm in diameter.

3.2 Spatial variation of water content

Before each test, four locations (Fig. 3) in each tree specimen were measured to determine the water content

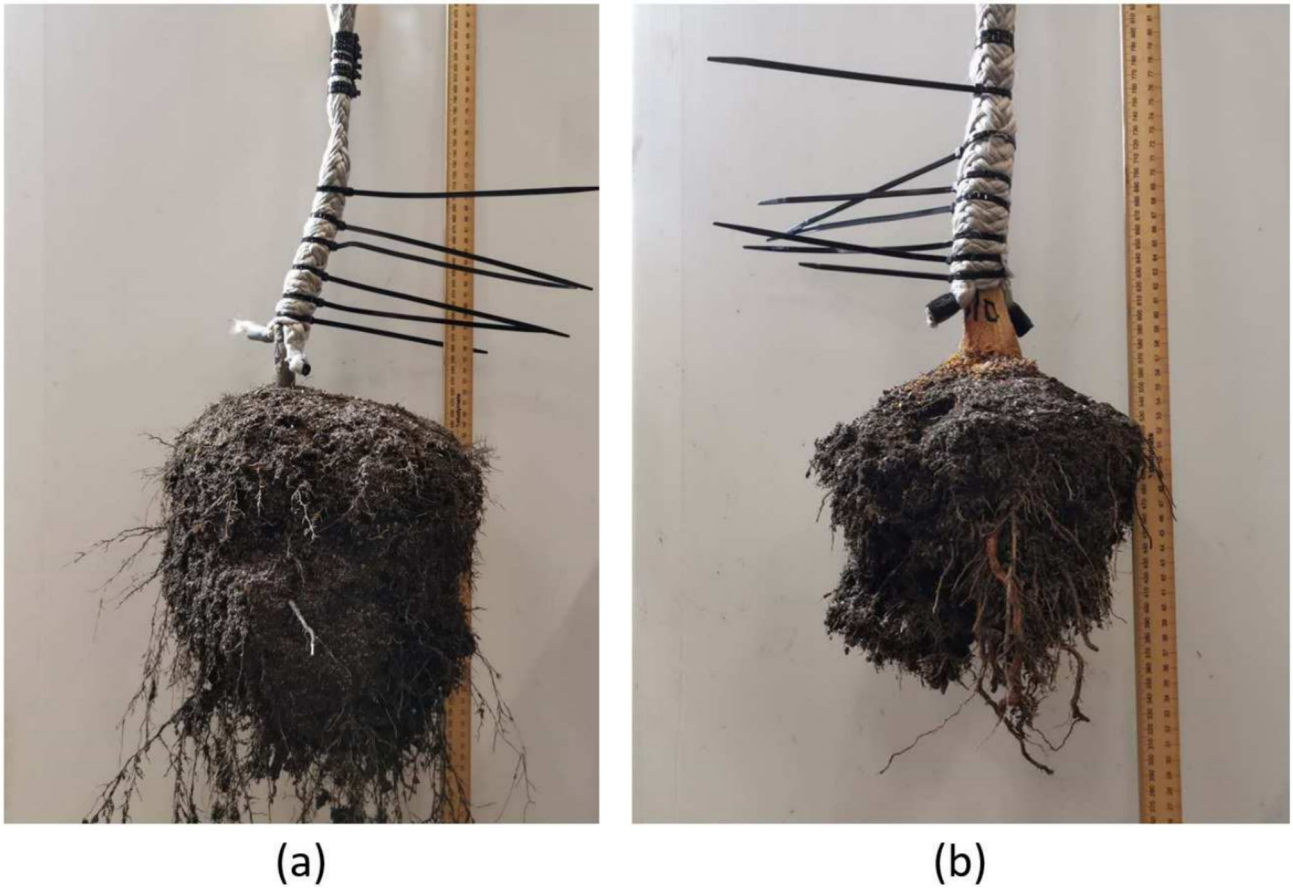

Fig. 5 Example of root bundles with **a** approximately cylindrical shape (*E. reticulatus*) and **b** less well-defined shape (*B. integrifolia*)

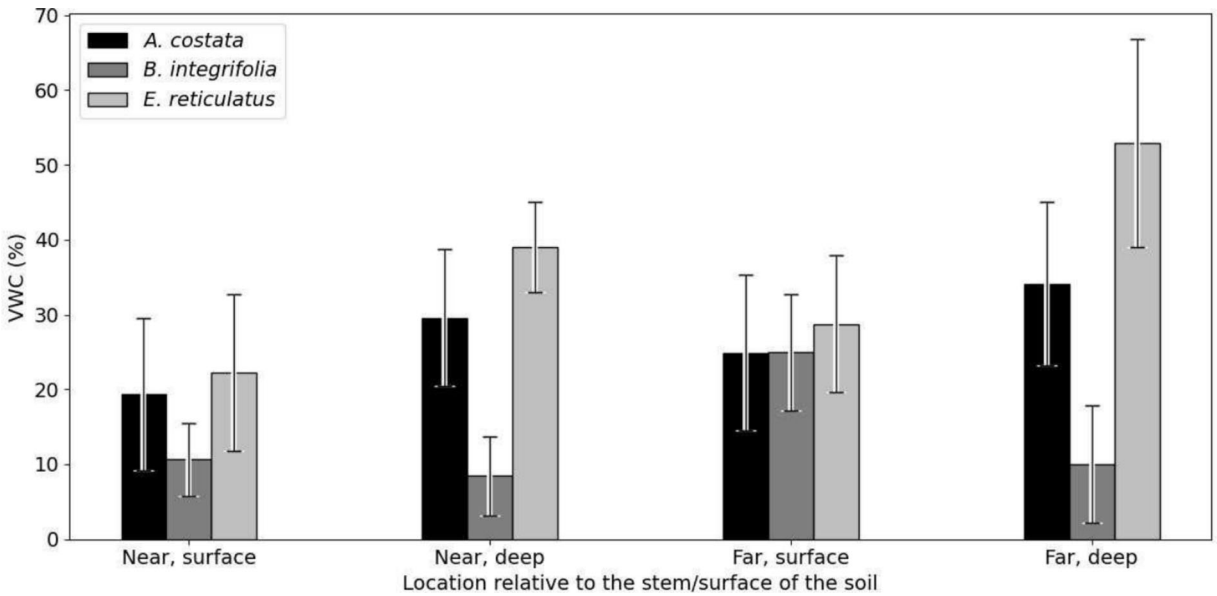

Fig. 6 Average VWCs measured at different locations around the root in the tree species with laboratory-based pull-out tests

distribution. The average values of suction and VWC for each tree species at these four measured locations are shown in Fig. 6.

The data presented in Fig. 6 exclude specimens that were inundated with water to simulate saturated conditions. The plants in these tests were submerged, so all VWCs in

the pot were close to the saturation value and hence did not reflect the water distribution due to transpiration and evaporation.

Figure 6 shows that the water content for *A. costata* and *E. reticulatus* were lowest near the surface and near the stem. The average VWCs of these two plants at the four locations exhibited similar patterns. Firstly, at the same distance from the stem, the water content at the base of the container exceeded that measured at the surface. In comparison, a difference is observed in the VWC of 'far' 'surface' for *B. integrifolia*, which exceeds its 'far' 'deep' equivalent. Possible reasons for this exception are discussed. The soil water content at the 'surface' generally decreases due to evaporation, seepage and transpiration from the surface roots, whereas the soil water content at 'deep' is primarily influenced by seepage through the bottom drainage holes and transpiration from the bottom roots. Hence, the lower water content at the surface of the container can be attributed to a strong evaporation [60, 61] in combination with fine surface lateral roots and seepage. In contrast, the water contents at the bottom were only affected by drainage and main roots.

Secondly, at the same depth, the water content increased as the distance from the stem increased. This may be attributed to the greater presence of roots near the stem, which promote greater transpiration and water absorption [32, 79]. In comparison, another difference is observed in the 'near' 'deep' VWC of *B. integrifolia* exceeding its 'far' 'deep' counterpart. Given the similar anomaly in the 'deep' versus 'surface' data associated with *B. integrifolia*, this may be due to a measurement error in the far deep VWC for this plant or a local heterogeneity in the soil or plant.

The differences exhibited by *B. integrifolia* specimens may also be a result of different root architecture and spatial distributions. To start with, *B. integrifolia* has advanced proteoid root systems, which significantly increase the surface area in contact with the soil by more than 140 times [80]. This extensive development of the micro-root system enhances the absorption of nutrients and water [81, 82], leading to a decrease in VWC. This results in the VWC measurements of *B. integrifolia* being generally lower than those of other species.

Moreover, observations of the extracted root-soil bundle showed that, in contrast to other species where the root density was generally higher close to the stem, *B. integrifolia* specimens exhibited fine proteoid roots away from the main stem, even at the bottom of the container. The fine roots at the bottom of the container may be attributed to root overgrowth in the container [57], which leads to an increase of the root surface area and thus enhanced water absorption [61].

These results highlight the importance of understanding the spatial variation of water content (and hence suction) in the surrounding soil matrix in root reinforcement studies, particularly where a strong root system is present or drainage is limited. Poor sampling could lead to a significant discrepancy between the measured water content and the actual representative value. It is recommended to measure VWC at several locations of interest to better characterise the variation in water content and identify the representative water content. If the experimental investigation primarily focuses on identifying the root-reinforced slope strength, rather than the effects of suction, then a different approach may be beneficial. Using saturated specimens can help reduce the spatial variation of water content. This method may have the added advantage of being conservative, since it helps in identifying the minimum strength of the system, corresponding possibly to conditions of heavy precipitation.

3.3 Peak pull-out force versus water content and suction

The highest and lowest ambient temperatures during the experiments were 23.9°C and 17°C, respectively. The peak pull-out force of individual trees ($F_{pk\,individual}$) versus VWC and $F_{pk\,individual}$ versus s_{matric} are plotted in Fig. 7 (a) and (b). As mentioned earlier, the weight of the root biomass and attached soil (root-soil bundle) was subtracted from the peak pull-out force value presented in Fig. 7.

The graph clearly shows a continuous decrease in peak pull-out force as volumetric water content increases. Initially, this decrease is more pronounced at lower VWC levels, where the slopes of the trend lines are steep. As the VWC increases further, the slopes become progressively less steep, indicating a gradual reduction in the rate at which the force decreases. This trend suggests a diminishing impact of additional water content on the pull-out force as the soil approaches higher water saturation levels. s_{matric} is an indicator of the binding pressure exercised on the soil by surface tension of water and the resulting capillary bridges between particles. A positive linear relationship seems to exist between the pull-out force and s_{matric} across all three tree species. Based on observation of data in Fig. 7(a) and (b), a logarithmic regression ($F_{pk\,individual} = K_1 + K_2 * \ln(VWC)$, R^2_{log}) and a linear regression ($F_{pk\,individual} = K_3 + K_4 * s_{matric}$, R^2_{linear}) were applied to the two pairs of experimental results. The results and the goodness-of-fit (R^2) can be seen in Table 3.

The increase in peak force with suction observed between $F_{pk\,individual}$ and suction may be attributed to the increase of interfacial strength as a result of increase in soil effective stress [22].

It should be noted that, VWC and s_{matric} are interdependent [83]. This interdependence is typically represented

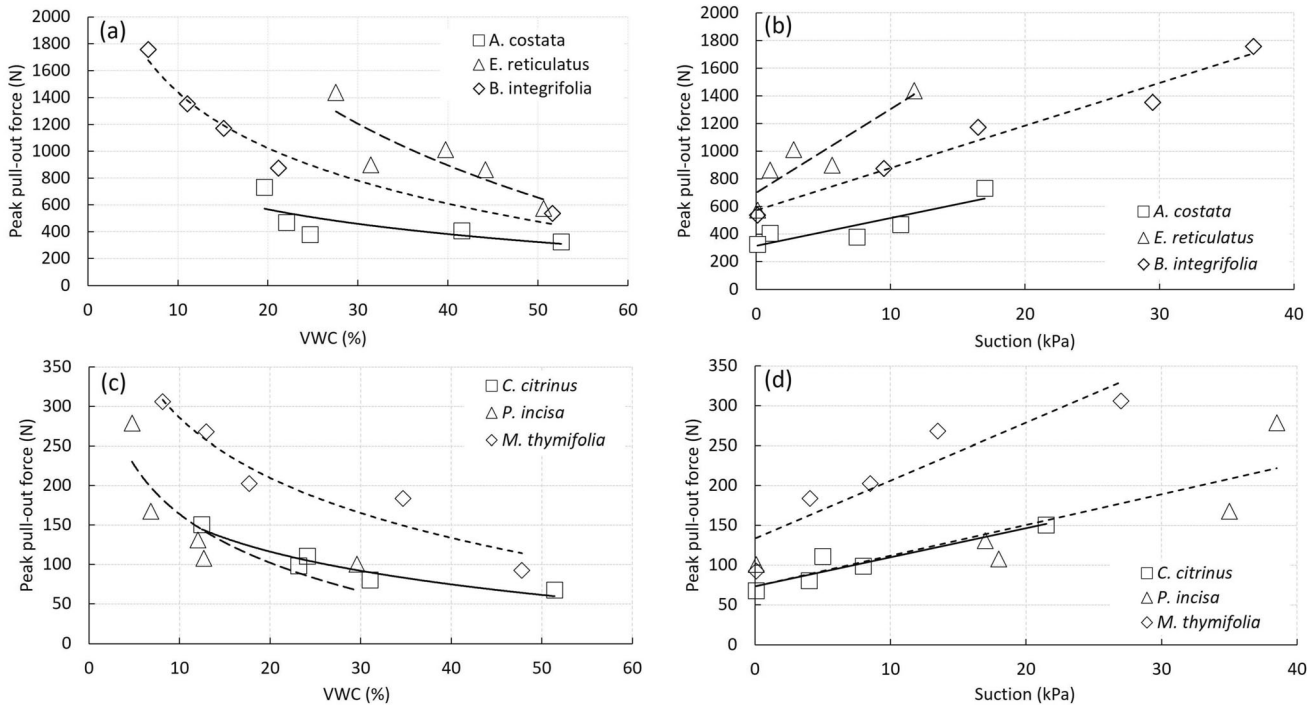

Fig. 7 Peak pull-out force against **a** average VWC for trees and **b** average suction for trees **c** average VWC for shrubs and **d** average suction for shrubs

Table 3 Linear regression expressions in peak pull-out force versus suction for the three tree species

	K_1	K_2	R^2_{log}	K_3	K_4	R^2_{linear}
A. costata	1363	−265.8	0.51	315.38	20.02	0.78
B. integrifolia	2816.3	−598.3	0.97	570.29	30.69	0.97
E. reticulatus	4872.9	-1078	0.73	698.37	60.70	0.82

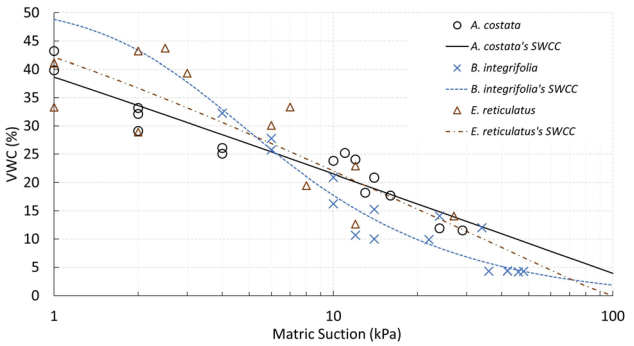

Fig. 8 VWC versuss matric suction from individual probes in experiments of the three tree species in semi-log scale

by the soil water characteristic curve (SWCC). Figure 8 presents the relationship between VWC and s_{matric} for the various specimens at four distinct probe locations in semi-log scale. As shown in Fig. 8, the SWCC of the root-soil bundle displayed a linear relationship in semi-log space with the lower-suction-end flattened. Such linear relationship in the semi-log space is consistent with data shown in 7. The fitting of the SWCC data uses the Van Genuchten [83] model yielded $\alpha = 2.6625$ 1/kPa, $n = 1.0002$ and $R^2 = 0.7514$ for *E. reticulatus*, $\alpha = 0.3274$ 1/kPa, $n = 1.8252$ and $R^2 = 0.9316$ for *B. integrifolia*, and $\alpha = 10.8554$ 1/kPa, $n = 1.0027$ and $R^2 = 0.8852$ for *A. costata*. As shown in Fig. 8, the variation in SWCC fitting parameters among the species is limited, and no significant differences were observed. This indicates a broadly consistent moisture retention behaviour in all three root-soil systems.

A similar process was employed to analyse the results from the shrub pull-out experiments, as displayed in Fig. 7(c) and (d). The regression equations for the relationship between peak pull-out force versus VWC and peak pull-out force versus s_{matric} are presented in Table 4. The

Table 4 Linear regression expressions in peak pull-out force versus water content and suction for the three shrub species

	K_1	K_2	R^2_{log}	K_3	K_4	R^2_{linear}
C. citrinus	295.7	−59.9	0.93	73.13	3.66	0.88
P. incisa	369.0	−89.1	0.72	73.31	3.86	0.67
M. thymifolia	538.1	−109.6	0.92	133.26	7.27	0.85

shrubs demonstrate a similar peak pull-out force against water content patterns as the trees. However, the values of $F_{pk\,individual}$ are significantly lower due to the smaller size of the shrub specimens.

The findings indicate that in situ experiments without control of the water content could yield inconsistent results. In practical engineering applications, this underscores the importance of implementing effective drainage strategies within bioengineered slope reinforcement initiatives. This approach is essential not only for preserving optimal soil moisture levels to maintain soil strength, but also for ensuring the efficacy of root reinforcement. For example, installing subsurface drainage systems, such as guided perforated pipes or gravel trenches near trees, can help control water accumulation and reduce the water content in the soil. Without such measures, tree reinforcement performance could fall below expectations, increasing the risk of slope failure.

3.4 Peak pull-out stress versus water content and suction

A summary of the bundle sizes for the plants is presented in Table 5. Similar to defining a root diameter for non-circular roots [26], the effective diameter is the average of the bundle's major and minor axes. The constraint ring confined the bundle size by restricting the failure surface to a cylindrical shape of a specific diameter; however, notable size differences among some root bundles were still observed.

Using this approach, the root-soil bundle can be likened to a micro-pile. In this analogy, the shaft capacity represents the frictional capacity at the interface between the root-soil bundle and the surrounding soil. The peripheral roots serve as binding agents between the bundle and neighbouring soil. With this normalisation, the peak pull-out stress ($\tau_{\mathrm{pk\,individual}}$) versus VWC and $\tau_{\mathrm{pk\,individual}}$ versus s_{ matric} are displayed in Fig. 9. As illustrated in Fig. 9 (a) and (c), a negative correlation between $\tau_{\mathrm{pk\,individual}}$ and VWC, which can be represented with a logarithmic regression. Notably, the relationship seems somewhat more linear, with a less distinct plateau in $\tau_{\mathrm{pk\,individual}}$ as VWC rises compared with the relationship between $F_{pk\,individual}$ and VWC.

Figure 9 (b) and (d) shows that the $\tau_{\mathrm{pk\,individual}}$ versus s_{matric} demonstrates a similar linear trend to the $F_{pk\,individual}$ versus s_{matric}. However, by accounting for bundle size, *A. costata* stands out as the most efficient species in providing pull-out resistance in trees. The regression expression between $\tau_{pk\,individual}$ and s_{matric} are shown in Table 6.

The normalisation of bundle size also appears to improve the regression model prediction for all the plants, except for *B. integrifolia* and *M. thymifolia*. It is also worth noting that after adjusting for bundle size, the regression models for *P. incisa* and *M. thymifolia* appear to converge, indicating a similar reinforcement performance.

By focusing on stresses instead of forces, the disparity in reinforcement performance between shrubs and trees narrows. The pull-out force varied from around 300-1600 N for trees and 50-300 N for shrubs. In comparison, the peak pull-out stress varied from around 3-12 kPa for trees and around 1-7 kPa for shrubs. This provides information on smaller scale applications, such as for soil erosion reinforcement on slopes. In such cases, shrubs can still be effective in providing additional soil strength for the shallow layer and their inter-species comparison is also enabled.

While this study has shown a good linear correlation between s_{matric} variation and peak pull-out stress, findings are still subject to certain limitations. Firstly, the bundle size measurement assumes a perfect elliptical cylinder shape. However, soil detachment during the pull-out process might diverge from this shape and might impact the measurement's accuracy. Currently, there is no definitive method to estimate the volume of detached soil accurately. Secondly, while the adopted method facilitates the measurement of a global average stress, it does not provide any insight into the actual stress distribution within the bundle.

Table 5 Bundle effective diameter for six species (measured in mm)

Species	Maximum	Minimum	Mean	Standard deviation
A. costata	155	110	126	17.5
B. integrifolia	245	200	219	17.8
E. reticulatus	260	235	248	9.8
C. citrinus	130	110	120	7.9
P. incisa	140	70	100	27.6
M. thymifolia	135	105	116	9.8

3.5 Pull-out experiment result and example root reinforcement model prediction

This study employed two root reinforcement models to illustrate the influence of VWC on the comparison between root reinforcement model performances and experimental results. The root counts within different diameter classes, located 100 mm from the stem as detailed in Table 2, served to estimate the root numbers at the bundle-soil interface. Given the counting frame's dimensions of 100 mm by 100 mm, the root density (total root number per m^2) for each diameter class was determined by multiplying the counted root number by 100. As the root diameter distribution was discrete, the median diameters

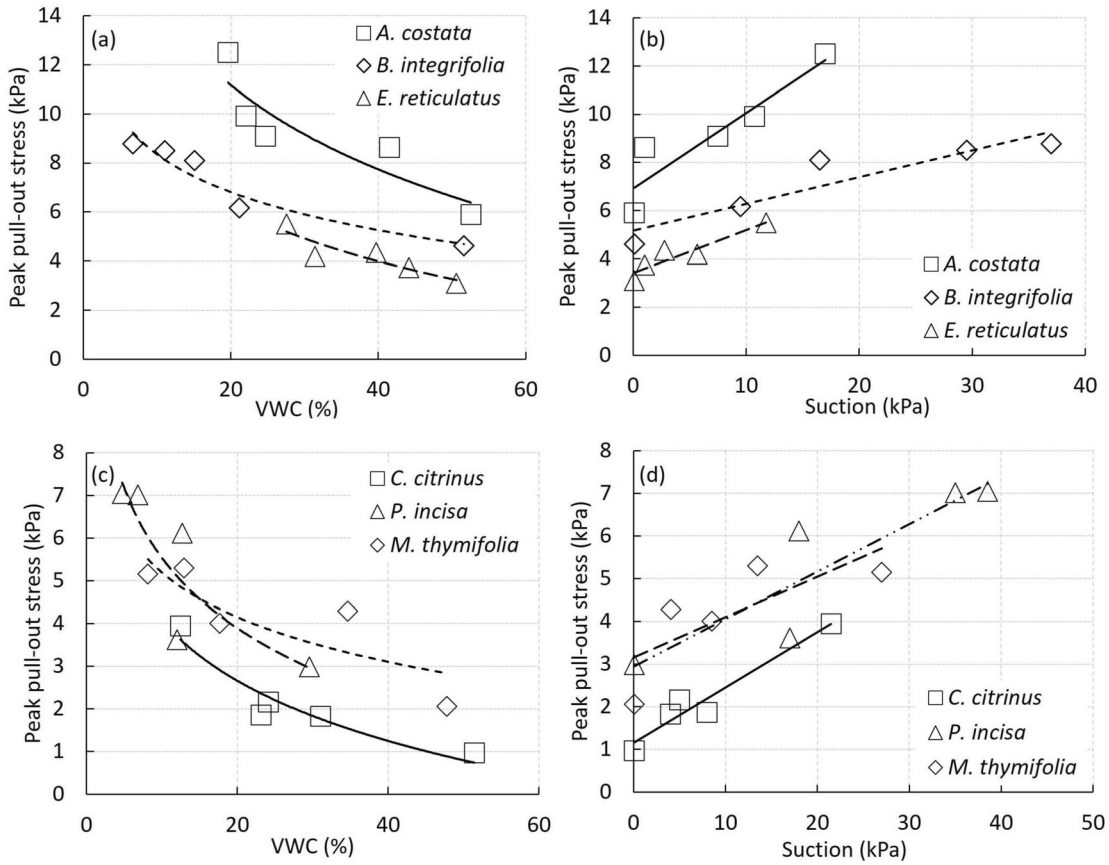

Fig. 9 Peak pull-out stress versus **a** VWC **b** suction for the trees and **c** VWC **d** suction for the shrubs

Table 6 Linear regression expressions in peak pull-out stress versus suction for the six species

	K_1	K_2	R^2_{log}	K_3	K_4	R^2_{linear}
A. costata	26.0	−5.0	0.80	6.92	0.31	0.86
B. integrifolia	13.5	−2.2	0.92	5.18	0.11	0.86
E. reticulatus	15.9	−3.2	0.82	3.42	0.18	0.88
C. citrinus	8.8	−2.0	0.91	1.15	0.13	0.94
P. incisa	11.0	−2.4	0.74	2.9	0.11	0.80
M. thymifolia	8.7	−1.5	0.70	3.15	0.09	0.58

Table 7 Tensile property parameters k_1, k_2, k_3, k_4 and the Weibull survival function parameters for RBMw k_5, k_6

Species	k_1	k_2	k_3	k_4	k_5	k_6
A. costata	19.05	1.17	5.76	0.89	1.18	2.82
B. integrifolia	10.41	1.15	1.78	1.16	1.20	4.18
E. reticulatus	24.5	1.04	3.28	1.05	1.13	3.36

for each class were used in the calculation of the total maximum force F_{max} in Eq. 1, same as the approach in Schwarz et al. [40]. The tensile properties employed in this investigation are summarised in Table 7, and the calibration functions for k_5 and k_6 are depicted in Fig. 10. The units for force and length in Eq. 1 and Eq. 2 involving k_1, k_2, k_3 and k_4 are Newtons (N) and millimetres (mm), respectively. k_5 and k_6 are dimensionless parameters.

The reinforcement performances of WWM and RBMw were calculated using Eq. 4 and Eq. 5 as force available per unit area, effectively stress. The two values were then compared to determine the k'' values, and all results are presented in Table 8.

This is similar to previous studies [34], where τ_{WWM} was notably higher than τ_{RBMw} (approximately 1.5−1.8 times, 0.556 to 0.667 in k'' values). Since neither model accounts for the effect of VWC, the reinforcement estimation remains unchanged irrespective of VWC variations. This can lead to significant discrepancies in model performance evaluation when compared with experimental results. For instance, Fig. 11 illustrates the $\tau_{pk\,individual}$ across various VWC conditions (as presented in Fig. 9), in comparison with τ_{WWM} and τ_{RBMw} for *B. integrifolia*.

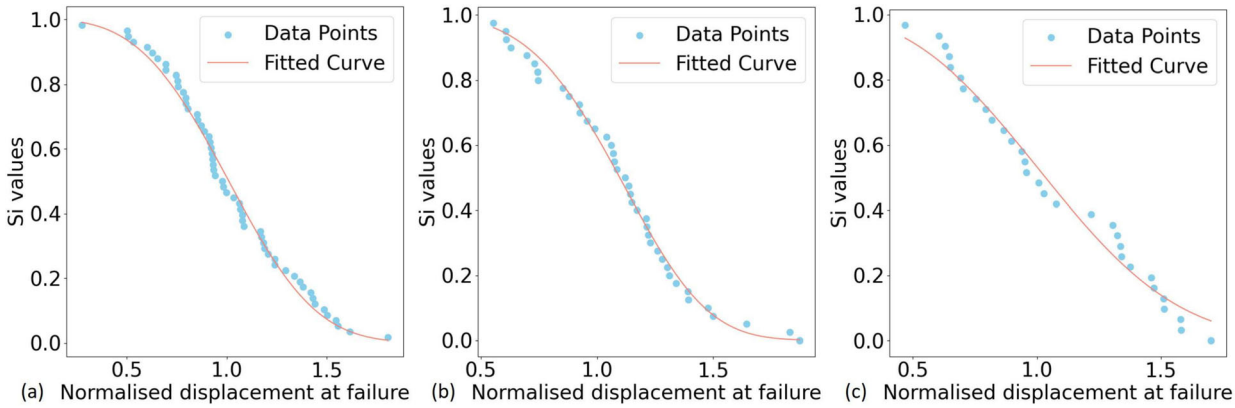

Fig. 10 Weibull survival function parameters calibration for RBMw of **a** *A. costata,* **b** *B. integrifolia and* **c** *E. reticulatus*

Table 8 WWM and RBMw reinforcement performance

Species	WWM (kPa)	RBMw (kPa)	k'' value
A. costata	43.6	23.8	0.55
B. integrifolia	13.7	9.3	0.68
E. reticulatus	49.2	28.8	0.59

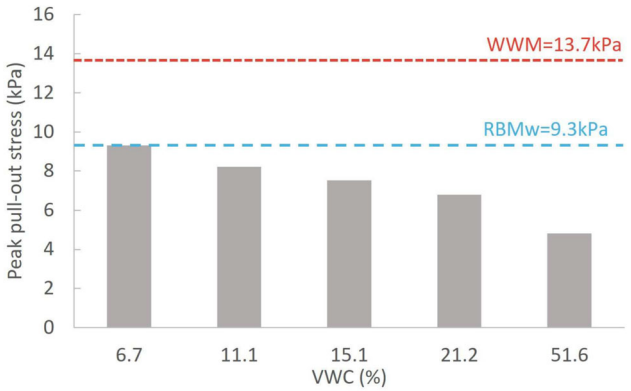

Fig. 11 Experimental peak pull-out stress versus VWC in comparison with WWM and RBMw predicted values for *B. integrifolia*

Discrepancies between root reinforcement model predictions and experimental results are common, as highlighted in a review study encompassing five species [34], a finding echoed in other studies [e.g. 4, 77]. Figure 11 demonstrates that τ_{WWM} consistently and significantly overestimates the peak pull-out stress. By contrast, RBMw estimated a peak pull-out stress of 9.3 kPa, which aligns with $\tau_{pk\,individual}$ at a VWC of 6.7% for *B. integrifolia*. However, as VWC increases, $\tau_{pk\,individual}$ decreases, thereby creating and widening the discrepancy. At a VWC of 51.6%, the RBMw prediction is twice the measured $\tau_{pk\,individual}$. For species *A. costata* and *E. reticulatus*, both τ_{WWM} and τ_{RBMw} surpass the experimental values, with τ_{WWM} having much higher overestimation. The consistent overestimation by both root reinforcement models compared with experimental results is common, as highlighted in a review study encompassing five species [34].

To more accurately quantify these differences and compare with existing literature, adjustment factors k''_{WWM} and k''_{RBMw} are employed, similar to k''. For this study, the adjustment factors were used to analyse the differences between root reinforcement models predicted values and experimentally acquired values. k''_{WWM} is defined as the ratio of $\tau_{pk\,individual}$ to τ_{WWM}, while k''_{RBMw} is the ratio of $\tau_{pk\,individual}$ to τ_{RBMw}. The values of k''_{WWM} and k''_{RBMw} for all three tree species under different VWC conditions are depicted in Fig. 12.

Figure 12 demonstrates that model prediction discrepancies can vary significantly with changes in soil water content. A lower k''_{WWM} and k''_{RBMw} indicate a greater overestimation. According to Fig. 12, k''_{WWM} ranges from 0.07 to 0.68, while k''_{RBMw} varies from 0.12 to 1.00. The model comparison study by Meijer [34] showed that k''_{WWM} typically fluctuates between 0.07−0.6 and k''_{RBMw} between 0.06−1.2, depending on the load sharing assumptions. The disparities between the applied models and experimentally

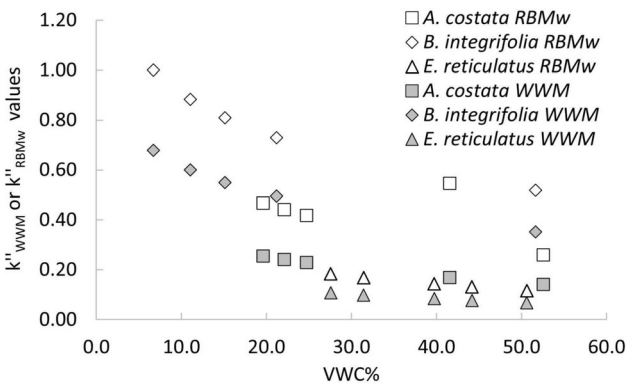

Fig. 12 k''_{WWM} and k''_{RBMw} values of the three selected tree species at different VWCs

measured values are consistent with and similar to these reported literature values.

The performance of root reinforcement model predictions, represented by k''_{WWM} and k''_{RBMw}, in this study, is constrained by various factors that also affect k''. These include assumptions regarding root orientation, root diameter distribution approximations [34], root spatial distribution [76] and root density approximations [77]. One important possible source of discrepancies is the inherent inability of FBMs to account for slippage [34]. Root-analogue pull-out experiments [22] showed that the interfacial strength decreases with increasing soil saturation. This suggests that root-soil interaction weakens as VWC increases, potentially leading to a shift from breakage to slippage failure as observed in Zhang et al. [31]. Such shift may invalidate the assumptions of tensile breakage failure in these models. Thus, the change in failure pattern might contribute to the variation in k''_{WWM} and k''_{RBMw} across different VWC levels.

It is worth noting that evaluating root reinforcement per unit area of roots, such as in Fan and Su [84], offers an alternative perspective on the performance evaluation. In this study, this approach involves dividing the total maximum force by the estimated total root cross-sectional area, and provides alternative insights into the effectiveness of root reinforcement.

In summary, the study outcomes reveal that discrepancies between root reinforcement model predictions and experimental results may be partly attributed to varying VWC. Measuring and controlling soil water content remains challenging in practical scenarios, as noted by Docker and Hubble [8]. Accurately recording VWC or soil suction is needed to refine model parameter calibration and enhance predictions in unsaturated soil conditions.

3.6 Australian native specie's soil reinforcement consideration

Specific studies in diverse ecological environments, such as the role of vegetation in mitigating landslides in Colorado, USA [85], and its effects on erosion control on the Loess Plateau, China [86], have demonstrated practical applications of root reinforcement in reducing slope instability. In the Australian context, previous studies have explored the stabilising effects of riparian genera like *Eucalyptus* on riverbanks [3, 87], focusing on mechanisms such as increased soil shear strength and progressive root failure. These studies underscore the importance of selecting vegetation that is tailored to local ecological and geological conditions.

By incorporating species native to Australian regions, this study aims to build on these understandings, offering area-specific insights into the bioengineering reinforcement of soils and contributing to the development of practical, regionally adapted insights. The selected species in this study are representative of native Australian trees found in diverse ecosystems along the east coast of Australia [50, 51, 55]. These species were selected because of their crucial ecological roles and their potential benefits for bioengineering. Discussions with horticulturists also underscored their growing incorporation into the application of urban forestry projects.

For example, *B. integrifolia* adapts well to poor soils, serves as a nectar source in heath ecosystems [53][88, 89], and helps preserve pollinators [90]. *E. reticulatus* offers blue berries that support local wildlife such as possums and birds, enhancing biodiversity [91]. *A. costata* and *E. reticulatus* are applied in urban areas to absorb effluent, improving safety and environmental health [52].

Based on the experimental observations from this study, *B. integrifolia* have a plate root structure as per Köstler [1968, as cited in 92], which is less effective against shallow landslides but increases overturn resistance [92–94] by increasing the distance of the lever arm during the uprooting [95]. Hence, planting *B. integrifolia* on the toe of a slope may better resist erosion or overturning events such as storms or debris flows. *A. costata* demonstrated the highest peak pull-out stress in various water contents (Fig. 9). This is in part due to the smallest diameter of the root-soil bundle (Table 5), a characteristic associated with a lack of fine root (Table 2). It has the potential to reinforce slope stability through anchorage, provided that roots are allowed to achieve substantial depth. *E. reticulatus* exhibits a root architecture that resembles a heart system, characterised by relatively thick vertical primary roots. It demonstrated the highest peak pull-out force among the three tree species (Fig. 7) examined. Consequently, *E. reticulatus* may be deemed suitable for the reinforcement of shallow slopes, attributed to its superior pull-out performance, robust root tensile properties (Table 7) and considerable ecosystem benefits.

4 Conclusion

This study conducted a series of pull-out experiments on six native Australian flora species (*A. costata*, *B. integrifolia*, *E. reticulatus*, *P. incisa*, *C. citrinus* and *M. thymifolia*) under varying water content conditions, thereby expanding the database on the root reinforcement performance of native Australian trees. The findings reveal a significant impact of VWC on root reinforcement performance across all species, with pull-out force diminishing as VWC increases. The relationship between VWC, soil

suction and pull-out force was observed, noting a roughly linear increase in pull-out force with increasing suction.

Furthermore, the study employed an innovative approach by making an analogy to soil nails or piles and normalising pull-out force against the peripheral surface area of observed root-soil bundles, defining this as pull-out stress. This normalised measure followed the same relationship with VWC and suction as the pull-out force. Interestingly, the ranking of species performance shifted, with *A. costata* exhibiting the highest pull-out stress due to its smaller root-soil bundle.

To complement these results and assess the influence of soil water content, two prevalent root reinforcement models, WWM and RBMw, were applied using the measured root tensile properties for three of the tree species. A close alignment was found between the RBMw model's estimated peak pull-out stress and the experimental results at a VWC of 6.7% for *B. integrifolia*. However, discrepancies between the model predictions and experimental measurements widened with increasing VWC, a trend also noted in *A. costata* and *E. reticulatus*. This underscores the importance of controlling and recording soil water content in such experiments.

Additionally, the study highlighted the impact of spatial variation in sampling, demonstrating that inadequate sampling can lead to substantial discrepancies between measured and actual representative water content values. This finding emphasises the necessity for rigorous sampling methods in root reinforcement research.

Future research involving in situ experiments, in comparison with laboratory tests, could significantly enhance the evidence base and improve the credibility of laboratory testing protocols. Moreover, conducting studies on mature specimens of native Australian trees, including those not previously examined, would broaden our understanding of species' suitability for bioengineering applications. A deeper insight into root spatial distribution is also essential for enhancing root reinforcement model predictions. More broadly, future investigations should dedicate attention to the development of a public database that catalogues critical plant properties, like root tensile strength, essential for predicting the performance of plant-reinforced soils. Establishing uniform guidelines for data collection, particularly regarding the measurement of soil water content, is also crucial.

Acknowledgements The authors express their gratitude to Prof. David Airey, Mr. Ross Barker and Dr. Matthew Pye for their critical advice and contributions to the experiment design, data analysis and plant selection. Special thanks are extended to horticulturalists Mr. Dave Bateman and Ms. Sienna Lawrence for their expertise in horticulture. Acknowledgement is given to the Centre of Geotechnical Research and The Sydney Centre in Geomechanics and Mining Materials at The University of Sydney for their support.

Funding Open Access funding enabled and organized by CAUL and its Member Institutions.

References

1. Abernethy B, Rutherfurd I (2001) The distribution and strength of Riparian Tree roots in relation to Riverbank reinforcement. Hydrol Proces 15:63–79. https://doi.org/10.1002/hyp.152
2. Amoroso G, Frangi P, Piatti R, Ferrini F, Fini A, Faoro M (2010) Effect of container design on plant growth and root deformation of littleleaf Linden and field Elm. HortScience 45(12):1824–1829
3. Anderson CJ, COUTTS MP, RITCHIE RM, CAMPBELL DJ (1989) Root extraction force measurements for Sitka Spruce. Forestry: An Int J For Res 62(2):127–137. https://doi.org/10.1093/forestry/62.2.127. (**Accessed 2022-12-20**)
4. Australian National Botanic Gardens: Botanical Information - Australian Plant Information. Publisher: Australian National Botanic Gardens, Parks Australia (2016). https://www.anbg.gov.au/plantinfo/ Accessed 2022-12-10
5. De Baets S, Poesen J, Reubens B, Wemans K, De Baerdemaeker J, Muys B (2008) Root tensile strength and root distribution of typical Mediterranean plant species and their contribution to soil shear strength. Plant and Soil 305:207–226. https://doi.org/10.1007/s11104-008-9553-0
6. Bischetti GB, Chiaradia EA, Epis T, Morlotti E (2009) Root cohesion of forest species in the Italian Alps. Plant and Soil 324(1):71–89. https://doi.org/10.1007/s11104-009-9941-0. (**Accessed 2022-11-19**)
7. Bischetti GB, Chiaradia E, Simonato T, Speziali B, Vitali B, Vullo P, Zocco A (2005) Root strength and root area ratio of forest species in lombardy (Northern Italy). Plant and Soil 278:31–41
8. Boldrin D, Leung AK, Bengough AG (2018) Effects of root dehydration on biomechanical properties of woody roots of Ulex europaeus. Plant and Soil 431(1):347–369. https://doi.org/10.1007/s11104-018-3766-7. (**Accessed 2023-03-29**)
9. Burrall M, DeJong JT, Martinez A, Wilson DW (2020) Vertical pullout tests of orchard trees for bio-inspired engineering of anchorage and foundation systems. Bioinsp Biomimet 16(1):016009. https://doi.org/10.1088/1748-3190/abb414. (**Publisher: IOP Publishing. Accessed 2022-10-03**)
10. Clemson A (1985) Honey and Pollen Flora. Australian land series. Inkata Press [for] Dept. of Agriculture, New South Wales, Melbourne
11. Cofie P, Koolen AJ (2001) Test speed and other factors affecting the measurements of tree root properties used in soil reinforcement models. Soil and Tillage Res 63(1):51–56. https://doi.org/10.1016/S0167-1987(01)00225-2. (**Accessed 2022-11-19**)
12. Coutts MP (1983) Root Architecture and Tree Stability vol. 71

13. Danjon F, Stokes A, Bakker M (2013) Root Systems of Woody Plants. In: Plant Roots: The Hidden Half, Fourth Edition, pp. 29–1. https://doi.org/10.1201/b14550-34 . Journal Abbreviation: Plant Roots: The Hidden Half, Fourth Edition
14. Dinkelaker B, Hengeler C, Marschner H (1995) Distribution and function of proteoid roots and other root clusters. Botanica Acta 108(3):183–200. https://doi.org/10.1111/j.1438-8677.1995.tb00850.x. (**Accessed 2023-07-01**)
15. Docker BB, Hubble TCT (2008) Quantifying root-reinforcement of river bank soils by four Australian tree species. Geomorphology 100(3):401–418. https://doi.org/10.1016/j.geomorph.2008.01.009. (**Accessed 2022-12-20**)
16. Docker BB (2003) Biotechnical engineering on alluvial riverbanks of southeastern Australia: A quantified model of the earth-reinforcing properties of some native riparian trees
17. Eby P (2016) Planting to conserve threatened nomadic pollinators in NSW. The State of NSW and Office of Environment and Heritage
18. Elliot WR, Jones DL (1980) Encyclopaedia of Australian Plants Suitable for Cultivation. Lothian Publishing, Melbourne
19. Ennos AR (1993) The scaling of root anchorage. J Theoret Biol 161(1):61–75. https://doi.org/10.1006/jtbi.1993.1040. (**Accessed 2022-12-20**)
20. Fan C-C, Lu JZ, Chen HH (2021) The pullout resistance of plant roots in the field at different soil water conditions and root geometries. CATENA 207:105593. https://doi.org/10.1016/j.catena.2021.105593. (**Accessed 2022-12-30**)
21. Fan C-C, Su C-F (2008) Role of roots in the shear strength of root-reinforced soils with high moisture content. Ecol Eng 33(2):157–166. https://doi.org/10.1016/j.ecoleng.2008.02.013. (**Accessed 2022-12-30**)
22. Galpathage SG (2017) Experimental and numerical study of root reinforcement and suction in soil stabilisation. PhD thesis, University of Wollongong, University of Wollongong
23. Garg A, Coo JL, Ng CWW (2015) Field study on influence of root characteristics on soil suction distribution in slopes vegetated with Cynodon dactylon and Schefflera heptaphylla. Earth Surface Proces Landform 40(12):1631–1643. https://doi.org/10.1002/esp.3743. (**Accessed 2023-07-16**)
24. Garg A, Leung AK, Ng CWW (2015) Comparisons of soil suction induced by evapotranspiration and transpiration of S. Heptaphylla. Canad Geotech J 52(12):2149–2155. https://doi.org/10.1139/cgj-2014-0425
25. Ge S (2003) HYDROLOGY | Ground and Surface Water. In: Holton, J.R. (ed.) Encyclopedia of Atmospheric Sciences, pp. 973–979. Academic Press, Oxford. https://doi.org/10.1016/B0-12-227090-8/00171-8 . https://www.sciencedirect.com/science/article/pii/B0122270908001718 Accessed 2023-07-16
26. Genet M, Stokes A, Salin F, Mickovski SB, Fourcaud T, Dumail J-F, Beek R (2005) The influence of cellulose content on tensile strength in tree roots. Plant and Soil 278(1):1–9. https://doi.org/10.1007/s11104-005-8768-6
27. Van Genuchten M (1980) A closed-form equation for predicting the hydraulic conductivity of unsaturated soils. Soil Sci Soc Am J 44:892–898
28. Giadrossich F, Cohen D, Schwarz M, Seddaiu G, Contran N, Lubino M, Valdés-Rodríguez OA, Niedda M (2016) Modeling bio-engineering traits of Jatropha curcas L. Ecol Eng 89:40–48. https://doi.org/10.1016/j.ecoleng.2016.01.005. (**Accessed 2022-11-27**)
29. Giadrossich F, Guastini E, Preti F, Vannocci P (2010) Experimental methodologies for the direct shear tests on soils reinforced by roots. Geol. Tec. Ambient. [J. Tech. Environ. Geol.] 4:67–76
30. Giadrossich F, Schwarz M, Cohen D, Cislaghi A, Vergani C, Hubble T, Phillips C, Stokes A (2017) Methods to measure the mechanical behaviour of tree roots: a review. Ecol Eng 109:256–271. https://doi.org/10.1016/j.ecoleng.2017.08.032. (**Accessed 2022-11-14**)
31. Giadrossich F, Schwarz M, Cohen D, Preti F, Or D (2013) Mechanical interactions between neighbouring roots during pullout tests. Plant and Soil 367(1):391–406. https://doi.org/10.1007/s11104-012-1475-1. (**Accessed 2022-11-27**)
32. Giambastiani Y, Preti F, Errico A, Sani L (2017) On the tree stability: pulling tests and modelling to assess the root anchorage. Procedia Environ Sci Eng Manag 4:207–218
33. Godt J, Coe J, Kean J, Baum R, Jones E, Harp E, Staley D, Barnhart W (2014) Landslides in the Northern Colorado Front Range Caused by Rainfall, September 11-13, 2013. https://doi.org/10.3133/fs20133114
34. Grierson PF, Attiwill PM (1989) Chemical characteristics of the proteoid root mat of Banksia integrifolia L. Austr J Botany 37(2):137–143. https://doi.org/10.1071/bt9890137. (**Publisher: CSIRO PUBLISHING. Accessed 2023-07-11**)
35. Griffith City Council: Working Towards Safe & Responsible On-Site Sewage Management Fact Sheet 11 (2022). https://www.griffith.nsw.gov.au/get-septicsmart Accessed 2022-12-10
36. Gurpersaud N, Vanapalli SK, Sivathayalan S (2013) Semiempirical method for Estimation of pullout capacity of grouted soil nails in saturated and unsaturated soil environments. J Geotech Geoenviron Eng 139(11):1934–1943
37. Gurpersaud N, Vanapalli SK, Sivathayalan S (2011) Pull-out capacity of soil nails in unsaturated soils. In: 14th Pan-American Conference on Soil Mechanics and Geotechnical Engineering 64th Canadian Geotechnical Conference, Toronto, Ontario, Canada
38. Hales TC, Cole-Hawthorne C, Lovell L, Evans SL (2013) Assessing the accuracy of simple field based root strength measurements. Plant and Soil 372(1):553–565. https://doi.org/10.1007/s11104-013-1765-2
39. Hatami K, Esmaili D (2015) Unsaturated soil-woven geotextile interface strength properties from small-scale pullout and interface tests. Geosynt Int 22:161–172. https://doi.org/10.1680/gein.15.00002
40. Hatami K, Khoury C, Miller G (2008) Suction-controlled testing of soil-geotextile interfaces. In: GeoAmericas 2008, the First Pan American Geosynthetics Conference & Exhibition, 262–271
41. Holliday I (2004) Melaleucas: a Field and Garden Guide, 2nd, ed. Reed New Holland Publishers, Frenchs Forest, N.S.W
42. Hubble TCT, Airey DW, Sealey HK, De Carli EV, Clarke SL (2013) A little cohesion goes a long way: estimating appropriate values of additional root cohesion for evaluating slope stability in the Eastern Australian highlands. Ecol Eng 61:621–632. https://doi.org/10.1016/j.ecoleng.2013.07.069. (**Accessed 2024-03-10**)
43. Hubble TCT, Docker BB, Rutherfurd ID (2010) The role of riparian trees in maintaining riverbank stability: a review of Australian experience and practice. Ecol Eng 36(3):292–304. https://doi.org/10.1016/j.ecoleng.2009.04.006. (**Publisher: Elsevier Ltd., Accessed 2023-02-18**)
44. Hubble TCT, Rutherfurd ID (2010) Evaluating the relative contributions of vegetation and flooding in controlling channel widening: the case of the Nepean River, southeastern Australia. Austr J Earth Sci 57(5):525–541
45. Jacobs MR (1955) Growth Habits of the Eucalypts. Commonwealth Forestry and Timber Bureau, Canberra. Publisher: Commonwealth Forestry and Timber Bureau. https://www.cabdirect.org/cabdirect/abstract/19550602567 Accessed 2022-12-10
46. Judd LA, Jackson BE, Fonteno WC (2015) Advancements in root growth measurement technologies and observation capabilities for container-grown plants. Plants 4(3):369–392. https://doi.org/10.3390/plants4030369. (**Number: 3 Publisher: Multidisciplinary Digital Publishing Institute. Accessed 2023-07-09**)

47. Khalilnejad A, Ali F, Osman N (2012) Contribution of the root to slope stability. Geotech Geol Eng 30:277–288. https://doi.org/10.1007/s10706-011-9446-5
48. Lamont BB (2003) Structure, ecology and physiology of root clusters - a review. Plant and Soil 248(1):1–19. https://doi.org/10.1023/A:1022314613217. (**Accessed 2023-07-11**)
49. Leung AK, Garg A, Coo JL, Ng CWW, Hau BCH (2015) Effects of the roots of Cynodon dactylon and Schefflera heptaphylla on water infiltration rate and soil hydraulic conductivity. Hydrol Proces 29(15):3342–3354. https://doi.org/10.1002/hyp.10452. (**Accessed 2023-07-16**)
50. Leung AK, Garg A, Ng CWW (2015) Effects of plant roots on soil-water retention and induced suction in vegetated soil. Eng Geol 193:183–197. https://doi.org/10.1016/j.enggeo.2015.04.017. (**Accessed 2023-07-16**)
51. Leung FTY, Yan WM, Hau BCH, Tham LG (2018) Mechanical pull-out capacity and root reinforcement of four native tree and shrub species on ecological rehabilitation of roadside slopes in hong kong. J Trop For Sci 30(1):25–38
52. Lin D-G, Huang B-S, Lin S-H (2010) 3-D numerical investigations into the shear strength of the soil-root system of Makino bamboo and its effect on slope stability. Ecol Eng 36(8):992–1006. https://doi.org/10.1016/j.ecoleng.2010.04.005. (**Accessed 2023-01-05**)
53. Liu Y, Gao J, Lou H, Zhang J, Cui Q (2011) The root anchorage ability of Salix alba vartristis using a pull-out test. Afri J Biotechnol 10(73):16501–16507 (**Number: 73. Accessed 2022-12-20**)
54. Mallett SD (2019) Mechanical behavior of fibrous root-inspired anchorage systems. PhD thesis, Georgia Institute of Technology, Georgia Institute of Technology (November). Accepted: 2020-01-14T14:46:37Z Publisher: Georgia Institute of Technology. https://smartech.gatech.edu/handle/1853/62304 Accessed 2023-01-08
55. Mao Z (2022) Root reinforcement models: classification, criticism and perspectives. Plant and Soil 472(1):17–28. https://doi.org/10.1007/s11104-021-05231-1. (**Accessed 2023-01-07**)
56. Mao Z, Saint-André L, Genet M, Mine F-X, Jourdan C, Rey H, Courbaud B, Stokes A (2012) Engineering ecological protection against landslides in diverse mountain forests: choosing cohesion models. Ecol Eng 45:55–69. https://doi.org/10.1016/j.ecoleng.2011.03.026. (**Accessed 2023-02-27**)
57. Masi EB, Segoni S, Tofani V (2021) Root reinforcement in slope stability models: a review. Geosciences 11(5):212. https://doi.org/10.3390/geosciences11050212. (**Number: 5 Publisher: Multidisciplinary Digital Publishing Institute. Accessed 2022-12-28**)
58. Meijer GJ (2021) A generic form of fibre bundle models for root reinforcement of soil. Plant and Soil 468(1):45–65. https://doi.org/10.1007/s11104-021-05039-z. (**Accessed 2022-12-28**)
59. Ng C, Leung A, Ni J (2019) Plant-Soil Slope Interaction. CRC Press, Boca Raton
60. Ng CWW, Woon KX, Leung AK, Chu LM (2013) Experimental investigation of induced suction distribution in a grass-covered soil. Ecol Eng 52:219–223. https://doi.org/10.1016/j.ecoleng.2012.11.013. (**Accessed 2023-07-16**)
61. Ng CWW, Zhang Q, Ni J, Li Z (2021) A new three-dimensional theoretical model for analysing the stability of vegetated slopes with different root architectures and planting patterns. Comput Geotech 130:103912. https://doi.org/10.1016/j.compgeo.2020.103912. (**Accessed 2022-12-29**)
62. Nilaweera NS, Nutalaya P (1999) Role of tree roots in slope stabilisation. Bullet Eng Geol Environ 57(4):337–342. https://doi.org/10.1007/s100640050056. (**Accessed 2022-12-30**)
63. Norris JE (2005) Root reinforcement by hawthorn and oak roots on a highway cut-slope in Southern England. Plant and Soil 278(1/2):43–53 (**Publisher: Springer. Accessed 2022-12-20**)
64. Northern Beaches Council: Native planting guide (2019). https://www.northernbeaches.nsw.gov.au/environment/native-plants/native-planting-guide Accessed 2022-12-10
65. Pollen N (2007) Temporal and spatial variability in root reinforcement of streambanks: accounting for soil shear strength and moisture. CATENA 69(3):197–205. https://doi.org/10.1016/j.catena.2006.05.004
66. Pollen N, Simon A (2005) Estimating the mechanical effects of riparian vegetation on stream bank stability using a fiber bundle model. Water Resour Res. https://doi.org/10.1029/2004WR003801
67. Rickli C, Graf F (2009) Effects of forests on shallow landslides - Case studies in Switzerland. For Snow and Landsc Res 82(1):33–44
68. Schwarz M, Cohen D, Or D (2011) Pullout tests of root analogs and natural root bundles in soil: experiments and modeling. J Geophys Res: Earth Surface. https://doi.org/10.1029/2010JF001753
69. Schwarz M, Giadrossich F, Cohen D (2013) Modeling root reinforcement using a root-failure Weibull survival function. Hydrol. Earth Syst. Sci. 17(11):4367–4377. https://doi.org/10.5194/hess-17-4367-2013
70. Schwarz M, Lehmann P, Or D (2010) Quantifying lateral root reinforcement in steep slopes-From a bundle of roots to tree stand. Earth Surface Proces Landform 35:354–367. https://doi.org/10.1002/esp.1927
71. Sharma S, Hussain S, Rai DV, Singh AN (2023) A comprehensive analysis on the ecosystem services of Elaeocarpus L. (Elaeocarpaceae): a review. J Phytol 15:12–37
72. Stokes A, Ball J, Fitter AH, Brain P, Coutts MP (1996) An experimental investigation of the resistance of model root systems to uprooting. Ann Botany 78(4):415–421. https://doi.org/10.1006/anbo.1996.0137
73. Stokes A, Douglas GB, Fourcaud T, Giadrossich F, Gillies C, Hubble T, Kim JH, Loades KW, Mao Z, McIvor IR, Mickovski SB, Mitchell S, Osman N, Phillips C, Poesen J, Polster D, Preti F, Raymond P, Rey F, Schwarz M, Walker LR (2014) Ecological mitigation of hillslope instability: ten key issues facing researchers and practitioners. Plant and Soil 377(1):1–23
74. Stokes A, Mattheck C (1996) Variation of wood strength in tree roots. J Exp Botany 47(5):693–699. https://doi.org/10.1093/jxb/47.5.693. (**Accessed 2023-09-25**)
75. Su L-J, Chan T, Yin J-H, Shiu Y, Chiu S (2008) Influence of overburden pressure on soil-nail pullout resistance in a compacted fill. J Geotech Geoenviron Eng 134:1339–1347
76. Tardío G, Mickovski SB (2016) Implementation of eco-engineering design into existing slope stability design practices. Ecol Eng 92:138–147. https://doi.org/10.1016/j.ecoleng.2016.03.036. (**Accessed 2022-12-14**)
77. The Australasian Virtual Herbarium: The Australasian Virtual Herbarium. Publisher: jurisdiction:Australian Government Departmental Consortium;corporateName:Council of Heads of Australasian Herbaria (2022). https://avh.ala.org.au/occurrences/search?q=taxa Accessed 2023-01-08
78. Tosi M (2007) Root tensile strength relationships and their slope stability implications of three shrub species in the Northern Apennines (Italy). Geomorphology 87(4):268–283. https://doi.org/10.1016/j.geomorph.2006.09.019. (**Accessed 2022-11-16**)
79. Vanapalli SK, Eigenbrod KD, Taylan ZN, Catana C, Oh WT, Garven EA (2010) technique for estimating the shaft resistance of test piles in unsaturated soils. Unsaturated Soils, Two Volume Set. Num Pages: 7

80. Vanapalli S, Taylan Z (2011) Estimation of the shaft capacity of model piles in a compacted fine-grained unsaturated soil. In: 14th Pan-American Conference on Soil Mechanics and Geotechnical Engineering 64th Canadian Geotechnical Conference, Toronto, Ontario, Canada. https://www.semanticscholar.org/paper/Estimation-of-the-shaft-capacity-of-model-piles-in-Vanapalli-Taylan/5b2f4a684fb5766bbf61b33bfce275f0153c2dcf Accessed 2023-02-18
81. Vergani C, Giadrossich F, Buckley P, Conedera M, Pividori M, Salbitano F, Rauch H, Lovreglio R, Schwarz M (2017) Root reinforcement dynamics of European coppice woodlands and their effect on shallow landslides: A review. Earth-Sci Rev 167:88–102. https://doi.org/10.1016/j.earscirev.2017.02.002. (**Accessed 2023-01-05**)
82. Waldron LJ (1977) The shear resistance of root-permeated homogeneous and stratified soil. Soil Sci Soc Am J 41(5):843–849. https://doi.org/10.2136/sssaj1977.03615995004100050005x. (**Accessed 2023-02-18**)
83. Waldron LJ, Dakessian S (1981) Soil reinforcement by roots: calculation of increased soil shear resistance from root properties. Soil Sci 132(6):427 (**Accessed 2023-02-26**)
84. Wang H, He Y, Shang Z, Han C, Wang Y (2018) Model test of the reinforcement of surface soil by plant roots under the influence of precipitation. Adv Mater Sci Eng 2018:3625053. https://doi.org/10.1155/2018/3625053
85. Woinarski JCZ, Connors G, Franklin DC (2000) Thinking honeyeater: nectar maps for the Northern Territory. Australia. Pacific Conserv Biol 6(1):61–80. https://doi.org/10.1071/pc000061. (**Publisher: CSIRO PUBLISHING Accessed 2023-07-13**)
86. Xu Y, Luo L, Guo W, Jin Z, Tian P, Wang W (2024) Revegetation changes main erosion type on the Gully-Slope on the Chinese loess Plateau under extreme rainfall: reducing Gully erosion and promoting shallow landslides. Water Resour Res 60(3):2023–036307. https://doi.org/10.1029/2023WR036307. (**Accessed 2025-01-28**)
87. Yang Y, Chen L, Li N, Zhang Q (2016) Effect of root moisture content and diameter on root tensile properties. PloS One 11(3):0151791. https://doi.org/10.1371/journal.pone.0151791
88. Yang M, Défossez P, Danjon F, Fourcaud T (2014) Tree stability under wind: simulating uprooting with root breakage using a finite element method. Ann Botany 114(4):695–709. https://doi.org/10.1093/aob/mcu122. (**Accessed 2022-12-21**)
89. Yang Q, Zhang C, Liu P, Jiang J (2021) The role of root morphology and pulling direction in pullout resistance of Alfalfa roots. Front Plant Sci 12:580825
90. Ye X, Wang S, Wang Q, Sloan S, Sheng D (2019) The influence of the degree of saturation on compaction-grouted soil nails in sand. Acta Geotech. https://doi.org/10.1007/s11440-018-0706-x
91. Zhang C, Liu Y, Liu P, Jiang J, Yang Q (2020) Untangling the influence of soil moisture on root pullout property of alfafa plant. J Arid Land. https://doi.org/10.1007/s40333-020-0017-6
92. Zhang C, Zhou X, Jiang J, Wei Y, Ma J, Hallett PD (2019) Root moisture content influence on root tensile tests of herbaceous plants. CATENA 172:140–147. https://doi.org/10.1016/j.catena.2018.08.012. (**Accessed 2022-11-19**)
93. Zhou Y, Wang X-S, Han P-F (2018) Depth-dependent seasonal variation of soil water in a thick vadose zone in the badain Jaran Desert. China. Water 10(12):1719. https://doi.org/10.3390/w10121719. (**Number: 12 Publisher: Multidisciplinary Digital Publishing Institute. Accessed 2023-07-16**)
94. Zhu J, El-Zein A, Airey DW, Miao G (2023) An experimental study on root-reinforced soil strength via a steel root analogue in unsaturated silty soil. Acta Geotechnica. https://doi.org/10.1007/s11440-023-01918-0. (**Accessed 2023-09-29**)
95. Zhu J, El-Zein A, Miao G (2024) The effect of diameter and moisture content on biomechanical properties of four native Australian trees. Plant and Soil. https://doi.org/10.1007/s11104-024-07136-1. (**Accessed 2024-12-26**)